Talanta 106 (2013) 266–280

Contents lists available at SciVerse ScienceDirect

Talanta

journal homepage: www.elsevier.com/locate/talanta

Optimization of a GC/MS procedure that uses parallel factor analysis for the determination of bisphenols and their diglycidyl ethers after migration from polycarbonate tableware

M.L. Oca [a], M.C. Ortiz [a,*], A. Herrero [a], L.A. Sarabia [b]

[a] Department of Chemistry, Faculty of Sciences, University of Burgos, Plaza Misael Bañuelos s/n, 09001 Burgos, Spain
[b] Department of Mathematics and Computation, Faculty of Sciences, University of Burgos, Plaza Misael Bañuelos s/n, 09001 Burgos, Spain

ARTICLE INFO

Article history:
Received 9 December 2011
Received in revised form
22 October 2012
Accepted 29 October 2012
Available online 2 November 2012

Keywords:
PTV-GC/MS
PARAFAC
Polycarbonate
Migrant
Bisphenol
Capability of detection

ABSTRACT

Bisphenol A (BPA), bisphenol F (BPF) and their corresponding diglycidyl ethers (BADGE and BFDGE) are simultaneously determined using a programmed-temperature vaporizer-gas chromatography/mass spectrometry (PTV-GC/MS) system. BPA is used in the production of polycarbonate (PC), whereas BADGE and BFDGE are for manufacturing epoxy resins. Several food alerts caused by the migration of this kind of substances from contact food materials have led to the harmonization of the European legislation in Commission Regulation (EU) No. 10/2011, in force from 14 January 2011. In consequence, the use of BPA has been prohibited in the manufacture of plastic infant feeding bottles from 1 May 2011 and from 1 June 2011 regarding the placing on the market and importation into the European Union. Recently, the French Parliament has decreed that the presence of BPA in any food containers will be banned. Similarly, the use and/or presence of BFDGE are not allowed.

In this work, a GC/MS method has been developed for the simultaneous determination of BPF, BPA, BFDGE and BADGE. For each one of the I samples that are analyzed, the abundance of J characteristic m/z ratios is recorded at K times around the retention time of each peak, so a data tensor of dimension $I \times J \times K$ is obtained for every analyte. The decomposition of this tensor by means of parallel factor analysis (PARAFAC) enables to: (a) identify unequivocally each analyte according to the maximum permitted tolerances for relative ion intensities, and (b) quantify each analyte, even in the presence of coeluents. This identification, based on the mass spectrum and the retention time, guarantees the specificity of the analysis. This specificity could fail if the total ion chromatogram (TIC) is considered when there is poor resolution between some peaks or whether interferents coelute.

With the aim of studying the effect of shortening the time of the analysis on the quality of the determinations while maintaining the specificity of the identifications, two of the heating ramps in the oven temperature program are changed according to a two-level factorial design. Each analyte is identified by means of a PARAFAC decomposition of a data tensor obtained from several concentration levels, in such a way that five figures of merit are calculated for each experiment of the design. The analysis of these figures of merit for the 16 objects (4 compounds $\times$ 4 heating ramps) using principal component analysis (PCA) shows that the shortest temperature program should be considered, since this is the one the best figures of merit for BPA and BFDGE (both banned) are achieved with. At these conditions and with probabilities of false positive and false negative fixed at 0.05, values of detection capability (CCβ) between 2.65 and 4.71 $\mu g\,L^{-1}$ when acetonitrile is the injection solvent, and between 1.97 and 5.53 $\mu g\,L^{-1}$ when acetone, are obtained.

This GC/MS method has been applied to the simultaneous determination of BPF, BPA, BFDGE and BADGE in food simulant D1 (ethanol–H_2O, 1:1 v/v), which had been previously in contact with PC tableware for 24 h at 70 °C and then pretreated by a solid-phase extraction (SPE) step. The migration of BPA from the new PC containers analyzed is confirmed, and values between 104.67 and 181.46 $\mu g\,L^{-1}$ (0.73 and 1.27 $\mu g\,L^{-1}$ after correction) of BPA have been estimated. None of the results obtained exceeds the specific migration limit of 600 $\mu g\,L^{-1}$ established by law for BPA in plastic food materials

Abbreviations: BPA, bisphenol A; BPF, bisphenol F; BADGE, bisphenol A diglycidil ether; BFDGE, bisphenol F diglycidyl ether; PC, polycarbonate; PTV-GC/MS, programmed temperature vaporizer-gas chromatography/mass spectrometry; PARAFAC, parallel factor analysis; PCA, principal component analysis; CCα, decision limit; CCβ, detection capability; LVI, large volume injection; CORCONDIA, core consistency diagnostic; SIM, selected ion monitoring; MSD, mass spectrometer detector; TIC, total ion chromatogram; SPE, solid-phase extraction; LS, least squares; LMS, least median of squares

* Corresponding author. Tel.: +34 947259571; fax: +34 947258831.
E-mail address: mcortiz@ubu.es (M.C. Ortiz).

0039-9140/$ - see front matter © 2012 Elsevier B.V. All rights reserved.
http://dx.doi.org/10.1016/j.talanta.2012.10.086

different from PC infant feeding bottles. Severe problems of coelution of interferents have been overcome using PARAFAC decompositions in the analysis of these food simulant samples.

© 2012 Elsevier B.V. All rights reserved.

1. Introduction

The optimization of GC/MS procedures is usually aimed to achieve the most intense and resolved peaks so as to yield determinations of the best analytical quality. Somehow, if the structure of the signals provided by the GC/MS instrumentation is considered, the figures of merit that determine the quality of an analytical procedure can be directly optimized [1] by means of multiway techniques.

Calibrations based on n-way data provided by modern chromatographic instruments are increasingly used in chemical analysis due to their applicability to numerous analytical techniques and their so-called "second-order advantage". This property makes these methods especially useful for quantifying and identifying analytes in complex samples where unknown interferents are present. This is of great interest in identifying and quantifying either banned substances or those for which a permitted limit has been established. Several reviews on this topic can be found in [2–5].

Among multiway techniques, parallel factor analysis (PARAFAC), which is a generalization of principal component analysis (PCA) for three-way data, has been applied in many occasions on GC/MS data. The use of PARAFAC has successfully helped to solve frequent problems such as coelution of either compounds whose mass spectra are quite similar to that of the analyte of interest, or of unknown substances [6]; simultaneous optimization of solid-phase microextraction and derivatization stages [1,7]; or building overall calibration models to obtain robust analytical procedures to identify and quantify compounds in a single analysis [8].

BPA and BPF are widely used in the synthesis of resins and plastics [9,10] with multiple industrial applications, such as the production of lacquers, the inner coating of food cans and thermal paper [11]. Furthermore, BPA is used in the production of polycarbonate (PC), the chosen polymer to manufacture food containers, such as non-returnable bottles, feeding bottles, etc. On the other hand, BADGE and BFDGE are intermediates in the manufacturing of epoxy resins to produce lacquers in food cans [12].

It has been reported that trace amounts of these compounds can be released into food from plastic materials and articles intended to come into contact with food [13–17]. In consequence, the European Union has established specifications for these substances and restrictions of use, in addition to migration limits to ensure the safety of the food contact materials. The specific migration limit applicable in particular for BPA, expressed in mg BPA per kg food, is 0.6 (Commission Regulation (EU) No. 10/2011 [18]). However, the use of BPA has been prohibited in the manufacture of plastic infant feeding bottles from 1 May 2011 and from 1 June 2011 regarding the placing on the market and importation into the European Union, respectively (Commission Implementing Regulation (EU) No. 321/2011). Recently, the French Parliament has decreed that the presence of BPA in any food containers will be banned from 1 January 2014. Similarly, the use and/or presence of BFDGE in the production of materials and articles are also prohibited (Commission Regulation (EC) 1895/2005).

Identification and quantification of these compounds are usually carried out by means of chromatography coupled to mass spectrometry, both LC/MS and GC/MS. But other methods using LC coupled to fluorescence or electrochemical detection, as well as immunochemical methods, are also used [17,19]; however, the identification of compounds in these cases is only based on retention times, so the possibility of interference from other electrochemically active, absorbent or fluorescent substances may produce false positives; in this situation, a different method for confirmation would be necessary. The LC/MS analysis of BPA in food is exclusively performed using electrospray ionization and atmospheric pressure chemical ionization, both in negative mode [19–21]. Extracts of BPA in water and in different concentrations of ethanol in water [22] and in acetic acid [23] used as food simulants were also directly analyzed by reverse-phase HPLC. BPA can be detected underivatized in water by GC/MS [24,25], but sensitivity can be improved using preconcentration, liquid–liquid extraction and derivatization [26–28]. Derivatization leads to sharper peaks for BPA and consequently to a better separation from other analytes and coextracted matrix components, so higher sensitivity is achieved. Silylation and acetylation are the most used derivatization procedures, among other possibilities [29,30]. Large volume injection (LVI) techniques [31,32] can be an alternative to derivatization stages, which make analyses difficult and time-consuming. Chromatographic systems equipped with a programmed-temperature vaporizer (PTV) inlet permit this kind of sample injection, which improves the sensitivity of analytical procedures.

In this paper, an optimization procedure applied when the PARAFAC technique is used for multiresidue analyses is described. This procedure was applied to the determination of BPA, BPF and their diglycidyl ethers (BADGE and BFDGE). With the aim of studying the effect of some operating chromatographic conditions on the quality of the determinations and identifications of several compounds, various parameters in the oven temperature program were changed according to a two-level (30 and 6 $^{\circ}C\,min^{-1}$) factorial design. In order to compare the results obtained at the different operating conditions, five figures of merit were calculated for each analyte from a calibration curve based on a PARAFAC decomposition. Next, principal component analysis (PCA) was used to analyze the figures of merit for the four compounds altogether.

This procedure fulfilled the specifications set by the regulatory body of the European Union for the studied migrants without any derivatization step, saving time and reagents. PARAFAC decomposition made it possible to identify unequivocally (according to the maximum permitted tolerances for relative ion abundances) and quantify each analyte. This identification, based on mass spectra and retention times, guaranteed the specificity of the analysis.

In order to test the applicability of the procedure developed, the migration of BPA from some PC cups and glasses was studied. It is established in [18] that, for the demonstration of compliance for plastic materials and articles not yet in contact with food, like those evaluated in this work, it is possible to use food simulants representing the major physico-chemical properties exhibited by food. To be precise, food simulant D1 (50% ethanol) is assigned for milk and milk-based drinks by [18], which are some of the foodstuffs both cups and glasses are intended to come into contact with. After the migration test (24 h at 70 °C), food simulant samples were cleaned up and preconcentrated by solid-phase extraction (SPE) and analyzed following the GC/MS method optimized previously.

2. Methodology

2.1. PARAFAC model

When, for each one of the I analyzed samples, the abundance of J characteristic ions is recorded at K times around the retention

time of each peak using a GC/MS system, $I \times J \times K$ abundances (x_{ijk}) are obtained and arranged into three dimensions for every peak. This cube of experimental data is known as tensor $\underline{\mathbf{X}}$ with dimension $I \times J \times K$. The three ways (profiles or modes) of this tensor are named by their chemical meaning; in this case, the first one is the sample way, the second one is the spectral way, and the third one is the chromatographic way. In other words, the element x_{ijk} of the tensor represents the abundance of the j-th ion at the k-th time recorded for the i-th sample. Specific data analysis techniques are used to analyze the structured information contained in three-way tensors.

Considering an analyte, the abundance x_j of the j-th m/z ratio acquired by a mass spectrometer is

$$x_j = \chi \varepsilon_j, \; j = 1,2,...,J \tag{1}$$

where ε_j is a coefficient of proportionality between the concentration of analyte and the abundance. ε_j depends on the j-th m/z ratio. The vector consisting of these coefficients constitutes the spectral profile (the mass spectrum).

As the mass spectrometer is coupled to a chromatograph, the fraction of analyte eluting from the chromatographic column to the mass spectrometer changes over time. So the abundance recorded at the k-th time becomes

$$x_{jk} = \chi \varepsilon_j \tau_k, \; j = 1,2,...,J; \;\; k = 1,2,...,K \tag{2}$$

where τ_k can be considered as the fraction of analyte reaching the mass spectrometer at the time k. The vector of all τ_k's forms the chromatographic profile (chromatographic peak).

If F substances coelute, the abundance recorded at that time is the sum of the contributions of these F different compounds

$$x_{jk} \cong \sum_{f=1}^{F} \chi_f \varepsilon_{jf} \tau_{kf}, \; j = 1,2,...,J; \;\; k = 1,2,...,K \tag{3}$$

Finally, assuming that the f-th analyte appears at the same retention time in every chromatographic run, the abundance of the j-th m/z ratio in the i-th sample registered at the k-th retention time can be expressed as

$$x_{ijk} \cong \sum_{f=1}^{F} \chi_{if} \varepsilon_{jf} \tau_{kf}, \; i = 1,2,...,I; \;\; j = 1,2,...,J; \;\; k = 1,2,...,K \tag{4}$$

The set of all x_{ijk} experimental data forms the three-way array or tensor $\underline{\mathbf{X}}$.

A PARAFAC model of rank F for a data tensor $\underline{\mathbf{X}}$ can be expressed [33,34] as

$$x_{ijk} = \sum_{f=1}^{F} a_{if} b_{jf} c_{kf} + e_{ijk}, \; i = 1,2,...,I; \;\; j = 1,2,...,J; \;\; k = 1,2,...,K \tag{5}$$

where e_{ijk} are the residual errors of the model. As it can be observed, the PARAFAC model of Eq. (5) corresponds to the physical model of Eq. (4). PARAFAC is a generalization of bilinear PCA to three-way data first proposed by Cattell [35]. Assuming that the model of Eq. (5) is adequate for the acquired data, then the least squares solution is unique. In this case, it must coincide with the true underlying physical model of Eq. (4).

If the acquired data are trilinear, i.e. spectral and chromatographic profiles for every factor should be the same in all samples (differing only in their sizes), the least squares estimates for the unknown coefficients of Eq. (5) are unique [36]. This is the uniqueness property of PARAFAC, which means that each f-th factor is unequivocally characterized by its own sample, spectral and chromatographic profiles. Experimental trilinear data are suitable to be analyzed using PARAFAC, which makes it possible to identify compounds unequivocally by their spectral and chromatographic profiles. To measure the trilinearity degree of the experimental data tensor, the core consistency diagnostic index (CORCONDIA) has been developed [37].

Uniqueness is known in chemical analysis as the "second-order advantage". In this case, PARAFAC enables to estimate the mass spectrum and the chromatographic profile (both normalized) of an analyte even if another non-modeled substance coelutes. Therefore, it is possible to identify each analyte unequivocally using its own spectral profile, as established in some official regulations [38,39]. This property is useful for optimizing a GC/MS procedure because it makes it feasible to consider the effect on the identification and quantification of the analyte caused by changes in the experimental conditions of the procedure.

2.2. Capability of detection and decision limit

According to the ISO norm 11843–1:1997 [40], the detection capability or minimum detectable net concentration, x_d, is the true net concentration of the analyte in the material to be analyzed which will lead, with probability $1-\beta$, to the correct conclusion that the concentration in the analyzed material is different from that in the blank. The need of evaluating the probability of false positive, α, and of false negative, β, has also been recognized by IUPAC [41], and it is mandatory in the European Union [39] for the identification and quantification of residues that either are toxic or come from veterinary treatments in foodstuffs. Recently, the International Vocabulary of Basic and General Terms in Metrology [42] has adopted the same criterion to define the limit of detection. The classic definition for the detection limit as K times the standard deviation in the blank sample [43] only evaluates the probability of a false positive, but does not quantify the probability of a false negative explicitly; furthermore, it is independent of the slope of the calibration line. This in particular makes no sense, because the capability of detection of a method depends on the amount of the increase of the signal when the concentration of the analyte is increasing near the null concentration. A good revision of the evolution of the viewpoint of IUPAC can be found in the work by Currie [44]. IUPAC also advises against using a multiple of the standard deviation of a blank as quantification or detection limit, as indicated in note 3, page 37 in chapter 18 [41].

To consider the two probabilities of error correctly when evaluating the detection limit, the following one-tailed hypothesis test is posed about the presence of the analyte in the test sample:

$$\begin{aligned} &H_0 : x = 0 \text{ (there is not analyte in the sample,} \\ &\qquad \text{i.e. its concentration is null)} \\ &H_1 : x > 0 \text{ (there is analyte in the sample).} \end{aligned} \tag{6}$$

The probability of type I error, α, is the probability of affirming that there is analyte when there is not actually. That is, α is the probability of a false positive. The probability of type II error, β, is the probability of wrongly deciding from the experimental results that there is not analyte. Therefore, β is the probability of a false negative.

The definitions of decision limit and detection capability are generalized to decide if a sample is compliant or non-compliant with regard to a given reference value x_0. In this case, the decision limit is the concentration above which it can be decided with a statistical certainty of $1-\alpha$ that x_0 has been truly exceeded. The detection capability (CCβ) means the smallest content of the substance that may be detected, identified and/or quantified in a sample with an error probability of β (for a fixed error α) [39]. Therefore, for this case, the decision is formally defined by the

following one-tailed hypothesis test:

$$H_0 : x = x_0 \text{ (the concentration of analyte is equal to or less than } x_0)$$

$$H_1 : x > x_0 \text{ (the concentration of analyte is greater than } x_0). \quad (7)$$

Now the probabilities α and β are the probabilities of false non-compliance and false compliance, respectively. It is clear that the hypothesis test of Eq. (6) is a particular case of that in Eq. (7) when $x_0=0$.

The detection limit is a concentration, but analytical methods provide signals; thus, the calibration curve must be taken into account, because this is the way of transforming the detection signal into concentration. The solution in the univariate case when the linear calibration model is used appears in [45,46].

The increasing use of multivariate calibrations based on linear (PLS) or non-linear (polynomial, neural network) models, as well as of multiway calibrations such as those based on PARAFAC, makes a generalization of both concepts mentioned above necessary. The key is to use the regression "calculated concentration ($c_{calculated}$) vs true concentration (c_{true})"

$$y = \beta_0 + \beta_1 x + \varepsilon \quad (8)$$

The data (x_i, y_i), $i=1,\ldots, N$, are now the true values (x_i) of concentration and the corresponding values (y_i,) calculated from the calibration model. A detailed discussion about univariate calibration can be found in [47].

In the univariate case, the results are mathematically equivalent to those obtained with the regression "signal versus c_{true}" [48]. But the calculation of the capability of detection and the limit of decision by means of the regression "$c_{calculated}$ versus c_{true}" can be generalized to any calibration performed with signals of any order. This approximation is detailed in the tutorial of [49].

3. Experimental

3.1. Reagents and standard solutions

BPF (CAS no. 000620–92–8), BPA (CAS no. 000080–05–7), BPA-d_{16} (CAS no. 096210–87–6), BFDGE (CAS no. 002095–03–6) and BADGE (CAS no. 001675–54–3), all 97% or higher purity, were obtained from Sigma-Aldrich (Steinheim, Germany). Isocratic-grade-for-HPLC acetonitrile (ACN) and both gradient-grade-for-liquid-chromatography acetone and methanol were purchased from Merck (Darmstadt, Germany), while hydrochloric acid 37% AnalaR NORMAPUR and ethanol absolute GPR RECTAPUR® were from VWR International, LLC (Radnor, Pennsylvania, USA). Deionised water was obtained by using the Milli-Q gradient A10 water purification system from Millipore (Bedford, MA, USA).

Stock solutions of 100 mg L^{-1} in ACN and of 10 mg L^{-1} in acetone were prepared.

Optimization samples: a set of 8 standard solutions of BPF, BPA, BFDGE and BADGE of 0, 100, 200 (replicated), 400, 600 (replicated) and 800 μg L^{-1} (with 100 μg L^{-1} of BPA-d_{16} as internal standard) in ACN.

Validation samples: another set of 16 calibration standards of BPF, BPA, BFDGE and BADGE of 0, 2, 4, 6, 8, 10, 15, 20, 25, 30, 35, 40, 45, 50, 55 and 60 μg L^{-1} (with 8 μg L^{-1} of BPA-d_{16} as internal standard) in ACN.

For the analysis of simulant samples, calibration standards ranging from 0 to 90 μg L^{-1} of BPF, BPA, BFDGE and BADGE (with 10 μg L^{-1} of BPA-d_{16} as internal standard) were prepared in acetone. BPA standards with concentrations between 100 and 650 μg L^{-1} were also prepared for the quantification of the amount of this analyte migrated from the PC tableware.

3.2. Migration testing

The new PC cups (Cup 1 and Cup 2) and glasses (Glass 1 and Glass 2) were rinsed with deionised water several times before the migration test. After being filled with the simulant at room temperature (up to 250 mL in the case of the two cups and 200 mL for the two glasses), the containers were placed into a thermostatic water bath at 70 °C for 24 h. This interval of time would simulate a two year period of use if hot milk was considered to stay an average of 2 min in one of these containers once a day. At the end of the migration period, the cups and glasses were removed from the bath and allowed to reach room temperature for 12 h.

3.3. Solid-phase extraction procedure

The pH value of the samples was adjusted to 2.4 using hydrochloric acid 37% before they were pretreated by SPE. The final volume of each simulant sample was divided into 50 mL portions and kept in amber bottles, so subsamples spiked with BPF, BPA, BFDGE and BADGE at a concentration of either 200 or 400 ng L^{-1} and non-spiked subsamples were available from every container. Procedural blanks as well as five simulant samples at the 200 ng L^{-1} fortification level for assessing the repeatability of the method were also prepared in 50 mL glass flasks and acidified until pH 2.4.

SPE cartridges were conditioned without vacuum by adding 15 mL of methanol and, once 1 min had elapsed, equilibrated with 6 mL of Milli-Q water. After 2 min, the whole volume (50 mL) of every sample passed through the SPE cartridge at a flow rate of approximately 3 mL min^{-1} by adjusting vacuum. After every sample had been loaded, cartridges were rinsed with 3 mL of a methanol–water (10:90 v/v) mixture and dried under vacuum for 5 min. Elution of the analytes was performed using 6 mL of methanol, and then SPE cartridges were left to dry under vacuum for 30 min. Each eluate was collected in a 10 mL glass tube and evaporated to dryness at 40 °C using the miVac evaporator. Samples were redissolved in 400 μL of a solution containing 10 μg L^{-1} of BPA-d_{16} (internal standard), vortex-mixed for 35 s and transferred into an insert contained in a vial for GC/MS analysis.

3.4. GC/MS analysis

A volume of 10 μL was injected at a controlled speed of 3.5 μL s^{-1} (after each injection the syringe was washed firstly with acetone and next with ACN at the first part of the work, while two washings with acetone were performed throughout the analyses of simulant samples). The PTV inlet was operated in the solvent vent mode. During injection, the inlet temperature was held at 50 °C for 0.8 min, while the column head pressure was fixed at 7 kPa and the flow rate through the split vent was set at 20 mL min^{-1} (at a vent time of 0.5 min, the split valve was closed). Next, the inlet temperature was ramped at 10.8 °C s^{-1} up to 280 °C, which was held for 15 min. The split valve was re-opened 2 min after injection to purge the inlet at a vent flow of 47.4 mL min^{-1}. The oven temperature was maintained at 40 °C for 2 min, and then ramped at the corresponding heating rates set by an experimental design detailed in subsection "Optimization: experimental design" up to the end temperature of 280 °C. The carrier gas was maintained at a constant flow rate of 1.1 mL min^{-1}.

Analyses were performed in the electron ionization mode at 70 eV operating either in full scan (m/z ratios from 50 to 350) or in SIM mode. The SIM program used had four acquisition windows: window 1, for BPF peak, with an ion dwell time of 75 ms and 2.51 cycles s^{-1}; window 2, for BPA-d_{16} and BPA peaks, with an ion dwell time of 40 ms and 2.58 cycles s^{-1}; window 3, for BFDGE peak, with an ion dwell time of 75 ms and 2.50 cycles s^{-1};

and window 4, for BADGE peak, with an ion dwell time of 75 ms and 2.50 cycles s^{-1}. The electron multiplier was fixed at 1200 V, the ion source temperature at 230 °C, the GC/MS interface temperature at 300 °C, and the source vacuum at 10^{-5} Torr.

3.5. Instrumental

To control the temperature in the migration testing, a water bath equipped with an immersion thermostat Digiterm 200 (JP Selecta S.A., Barcelona, Spain) was employed. The vacuum manifold used for the SPE step was purchased from Waters Corporation (Milford, MA, USA). In order to reach the negative pressure required for the SPE, a laboratory vacuum pump for manifolds (Sartorius AG, Goettingen, Germany) was used. SPE cartridges were Oasis® HLB 200 mg/6 cc (Waters Corporation, Milford, MA, USA). The evaporation of the solvent in the eluates from the SPE stage was performed in a miVac Modular Concentrator (GeneVac Limited, Ipswich, UK), which consisted of a miVac Duo concentrator, a SpeedTrap™ and a Quattro pump. A ZX3 vortex mixer (VELP Scientifica, Usmate (MB), Italy) was used for homogenizing samples.

Analyses were carried out on an Agilent 7890A gas chromatograph coupled to an Agilent 5975C Mass Selective Detector (MSD). The injection system consisted of a septumless head and a PTV inlet (CIS 6 from GERSTEL GmbH & Co. KG, Germany) equipped with an empty multi-baffled deactivated quartz glass liner. LVI was carried out using the MultiPurpose Sampler (MPS 2XL from GERSTEL GmbH & Co. KG, Germany) with a 10 μL syringe. Analytical separations were performed on an Agilent HP-5MS Ultra Inert (30 m × 0.25 mm i.d., 0.25 μm film thickness) column. Helium was used as the carrier gas.

3.6. Software

MSD ChemStation E.02.01.1177 (Agilent Technologies, Inc.) and GERSTEL MAESTRO 1 (version 1.3.20.41/3.5) were used for data acquisition and processing with the help of the NIST mass spectral library [50]. A home-designed program enabled the transformation of the data exported from the GC/MS software into the appropriate format to build data tensors with MATLAB (version 7.9.0.529 (R2009b)). Principal component analysis and PARAFAC models were performed with the PLS_Toolbox 5.0 [51] for use with MATLAB. The least squares regressions were built and validated with STATGRAPHICS Centurion XVI [52]. Least median of squares regressions for the detection of outliers were carried out with PROGRESS [53]. Decision limit, CCα, and capability of detection, CCβ, were determined using the DETARCHI program [46], and CCα and CCβ at the maximum residue limit were estimated using NWAYDET (a program written in-house that evaluates the probabilities of false non-compliance and false compliance for n-way data).

4. Results and discussion

4.1. Initial approach: full scan mode

In order to develop a procedure to determine BPF, BPA, BFDGE and BADGE by means of GC/MS, initial analyses were carried out. At first, the following oven temperature program was set: the initial temperature (40 °C) was held for 2 min; then a 10 °C min^{-1} ramp to 175 °C, which was held for 2 min, followed by a 6 °C min^{-1} ramp to 280 °C, temperature maintained for 3 min. The total run time was 37.0 min. The mass spectrometer detector (MSD) was operated in full scan mode to permit the identification of compounds by comparing the acquired spectra with those of the NIST mass spectral library.

The chromatogram shown in Fig. 1a was obtained from the injection of a solution containing 500 μg L^{-1} of all these compounds along with the internal standard BPA-d_{16} and its subsequent analysis with this temperature program. In addition to the five expected peaks (1–5 in the fig.), other peaks appeared; one of them was identified as an isomer of BFDGE, while another as phthalates, which did not interfere in the analysis of the target compounds. In this sense, the chromatographic separation of BFDGE is harder than for the rest of the compounds, because the condensation reaction between phenol and formaldehyde, which may occur both in the *orto* and the *para* positions of the phenolic ring, results in the final formation of three isomers of BFDGE [54]. At these operating conditions, peak 5, corresponding to BADGE, appeared almost at 35 min. The total run time was too long.

Next, the oven temperature program was modified in the following way: 40 °C (maintained for 2 min); temperature increased at 60 °C min^{-1} to 150 °C (for 2 min), then at 30 °C min^{-1} to 280 °C (for 7 min). The total run time was 17.2 min. At these operating conditions, the chromatogram shown in Fig. 1b was obtained, where peaks appeared closer, as expected.

From a chromatographic point of view, the chosen temperature program should have been the last one, since it meant the shortest run time. However, this is not necessarily related to obtaining the best determinations from that temperature program, as the effect on the figures of merit of the analytes caused by changing the heating ramps in the oven program is unknown when PARAFAC is used. Finding this would be the main object of the first part of this work.

4.2. Initial approach: SIM mode

In order to achieve a higher sensitivity, the MSD no longer operated in full scan mode, but in SIM. The ions shown in Table 1

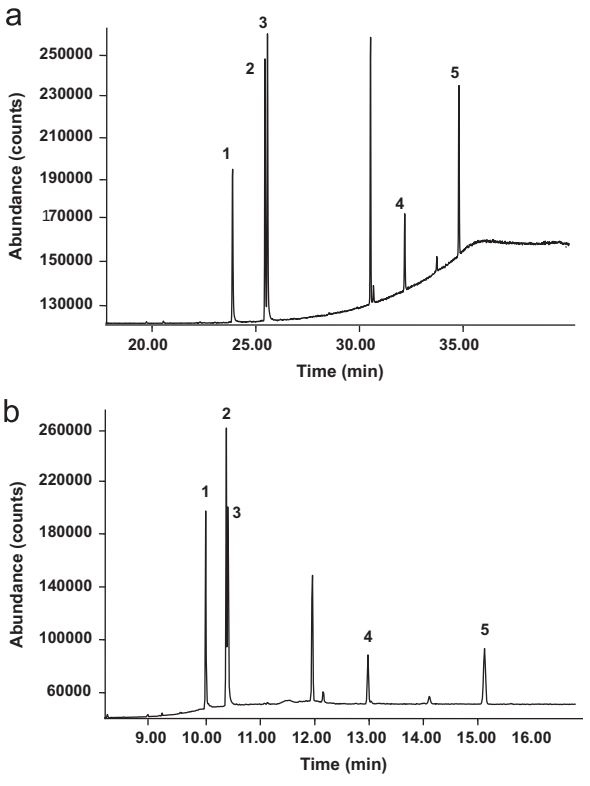

Fig. 1. Total ion chromatograms obtained in full scan mode from the injection of 500 μg L^{-1} of BPF, BPA-d_{16}, BPA, BFDGE and BADGE. Oven temperature programs were: (a) 40 °C (for 2 min), 10 °C min^{-1} 175 °C (for 2 min), 6 °C min^{-1} 280 °C (3 min); and (b) 40 °C (for 2 min), 60 °C min^{-1} 150 °C (2 min), 30 °C min^{-1} 280 °C (7 min). Peak labels: 1, BPF; 2, BPA-d_{16}; 3, BPA; 4, BFDGE; and 5, BADGE.

Table 1
Acquired ions (the most intense ones are in bold), abundance, relative abundance and tolerance intervals for the reference sample of 400 μg L^{-1} of the five compounds.

Analyte	m/z ratio	Abundance	Relative abundance (%)	Tolerance interval (%)
BPF	94	4018	15.83	(12.66–19.00)
	107	23760	93.60	(84.24–102.96)
	152	3948	15.55	(12.44–18.66)
	183	5616	22.12	(18.81–25.44)
	200	25384	100	–
BPA-d_{16}	125	14313	10.97	(8.78–13.17)
	224	130424	100	–
	242	26384	20.23	(17.20–23.26)
	244	422	0.32	(0.16–0.49)
BPA	91	11897	9.51	(4.76–14.27)
	107	5590	4.47	(2.23–6.70)
	119	21080	16.85	(13.48–20.22)
	213	125096	100	–
	228	22608	18.07	(14.46–21.69)
BFDGE (first peak)	107	2135	25.55	(21.72–29.38)
	181	5502	65.84	(59.26–72.43)
	197	8356	100	–
	279	344	4.12	(2.06–6.18)
	312	6438	77.05	(69.35–84.76)
BADGE	91	1313	2.62	(1.31–3.93)
	119	2006	4.00	(2.00–6.00)
	169	960	1.91	(0.96–2.87)
	325	50184	100	–
	340	7972	15.89	(12.71–19.06)

were chosen to identify the compounds from the spectra recorded previously. In the case of BFDGE, the characterization and quantification of the compound was carried out considering only the *p–p′* isomer.

At the sight of the TICs in Fig. 1a and b, it could be concluded that the peaks 2 and 3 were overlapped. As a consequence, as it is shown in Table 1, the diagnostic ions considered for identifying and quantifying the compound corresponding to the peak 2 (BPA-d_{16}) were specific and different from those chosen for BPA (peak 3), so both peaks were not actually overlapped in the spectral mode, and a real interference was thus not reflected.

The presence of the analytes was confirmed in accordance with the criteria collected in the Annex 2 of [55], where it is set, among other requirements, that the relative retention time of an analyte shall be the same as that of the calibration standard within a margin of ±0.5%. The relative retention time of every compound was calculated in relation to the absolute retention time of BPA-d_{16}, used as internal standard. In addition, the relative abundances of the detected ions shall correspond to those of the calibration standard within permitted maximum tolerances.

To establish the tolerance intervals, a sample with 400 μg L^{-1} of the five analytes was used as reference. So, after the recording of the mass spectrum of the analyte at its retention time, the percentage relative abundance of every m/z ratio in relation to the base peak (shown in bold in Table 1) was calculated. All the relative ion abundances determined for the different compounds and their relative retention times were within the estimated tolerance intervals, so all of them were unequivocally identified.

4.3. Optimization: experimental design

From the chromatograms shown in Fig. 1a and b, it was not possible to know which operating conditions led to the best figures of merit of the analytical procedure for all the analytes. This is a practical problem in multiresidue analysis, since the set

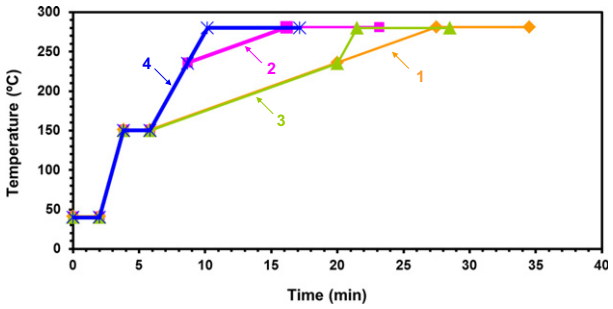

Fig. 2. Diagram of the studied oven temperature programs. Experiment 1, orange diamonds (Φ_3=6 °C min^{-1}; Φ_4=6 °C min^{-1}); Experiment 2, pink squares (Φ_3=30 °C min^{-1}; Φ_4=6 °C min^{-1}); Experiment 3, green triangles (Φ_3=6 °C min^{-1}; Φ_4=30 °C min^{-1}); and Experiment 4, blue asterisks (Φ_3=30 °C min^{-1}; Φ_4=30 °C min^{-1}). (For interpretation of the references to color in this figure legend, the reader is referred to the web version of this article.)

of operating conditions that optimize the figures of merit of an analyte does not necessarily lead to the simultaneous optimization of those of another one. This question could be approached by taking the structure of the acquired analytical signal into account: if the concentration of the compounds was varied, a data tensor would be available, which could be analyzed through the multiway techniques described previously. Moreover, it was of interest to study if the PARAFAC decomposition of that data tensor succeeded in extracting the chromatographic, spectral and sample profiles related to every analyte.

The aim of the design carried out was to find the optimum oven temperature program according to three criteria: (1) the capability of PARAFAC decomposition to resolve chromatographic peaks; (2) the quality of some figures of merit (CCα, CCβ, trueness, precision and relative errors) of the determinations; and (3) the total run time, which should be as short as possible.

Bearing in mind these considerations, two heating ramps (ϕ_3 and ϕ_4 in Fig. 2) in the oven temperature program were changed according to a two-level factorial design. Each ramp took the values shown in Table 2, which summarizes the four experiments in the experimental plan. The rest of the parameters in the oven temperature program were maintained as in the previous analyses. Fig. 2 shows the parameters in the oven temperature program related to these four runs (named experiments 1, 2, 3 and 4 throughout the text).

At the oven temperature conditions of each experiment, the chromatograms corresponding to the samples from 0 to 800 μg L^{-1} detailed in subsection "Reagents and standard solutions" were acquired. At experiments 1 and 3, a replicate of the 800 μg L^{-1} sample was also analyzed, so for every experiment of the design 8 or 9 analyses were carried out. After baseline correction, all the data matrices for every run were arranged together into a data tensor. Since for each of the I analyzed samples, the abundance of J characteristic m/z ratios was recorded at K times around the retention time of each peak, a data tensor of dimension $I \times J \times K$ was obtained for every analyte, except for BPA-d_{16} and BPA peaks, for which a common tensor was achieved. Therefore, four data tensors were available for each experiment.

4.4. Optimization: PARAFAC decomposition

PARAFAC decompositions of these data tensors were performed with the non-negativity constraint on two ways, as both chromatograms and spectra must always be positive. For BFDGE, the PARAFAC models had two factors for experiments 1, 2 and 3, with CORCONDIA values higher than 99%. The first of these factors was related to the *p–p′* isomer of BFDGE; the second factor was associated with a third isomer of BFDGE. That is, the use of this

Table 2
Experimental plan and figures of merit studied by using of PCA: residual standard deviation of the polynomial curves (s_{yx_load}), residual standard deviation of the accuracy line (s_{yx_accur}), decision limit for a nominal value of 600 μg L^{-1} and a probability of false non-compliance equal to 0.05 (CCα), mean (ERRORm) and standard deviation (ERRORstd) of the absolute values of relative errors.

Experimental plan			Object label	Figures of merit				
Experiment	Factors			s_{yx_load}	s_{yx_accur}	CCα (μg L^{-1})	ERRORm	ERRORstd
	Φ_3 (°C min^{-1})	Φ_4 (°C min^{-1})						
1	6	6	BPF_1	2.26×10^{-2}	13.74	621.2	3.68	3.94
			BPA_1	2.41×10^{-2}	12.91	619.9	3.57	3.43
			BFDGE_1	2.75×10^{-2}	10.73	616.5	1.75	0.88
			BADGE_1	5.82×10^{-2}	31.78	650.2	13.07	21.43
2	30	6	BPF_2	3.16×10^{-2}	12.28	620.3	3.75	5.06
			BPA_2	2.88×10^{-2}	11.55	619.1	2.55	2.48
			BFDGE_2	3.92×10^{-2}	16.83	627.7	3.26	1.79
			BADGE_2	3.75×10^{-2}	16.47	627.3	6.15	8.09
3	6	30	BPF_3	3.48×10^{-2}	15.01	623.0	3.67	4.24
			BPA_3	1.50×10^{-2}	8.56	613.2	2.48	2.95
			BFDGE_3	2.63×10^{-2}	16.49	625.1	2.60	1.58
			BADGE_3	7.11×10^{-2}	35.05	654.0	9.16	15.29
4	30	30	BPF_4	3.07×10^{-2}	13.58	622.5	3.98	5.30
			BPA_4	1.77×10^{-2}	8.74	614.5	2.67	3.04
			BFDGE_4	1.29×10^{-2}	6.96	611.5	1.76	2.57
			BADGE_4	4.93×10^{-2}	22.16	636.7	8.01	8.05

multiway technique made it possible to find a compound that could not be detected because it coeluted very close to the *p–p′* isomer. On the other hand, for BPF and BADGE, one-factor models were fitted for the four experiments of the design. For BPA-d_{16} and BPA, each PARAFAC model needed two factors, as expected, with CORCONDIA values of 100%. In all the cases, the loadings of the chromatographic, spectral and sample profiles were coherent.

By way of example, Fig. 3 shows the loadings of the PARAFAC model for BPA-d_{16} and BPA corresponding to experiment 4. The PARAFAC decomposition found two factors related to two different compounds, which were characterized by means of their respective chromatographic (Fig. 3a), spectral (Fig. 3b) and sample (Fig. 3c) profiles. The loadings of the chromatographic profile showed two close chromatographic peaks. It was confirmed that the relative retention time of both peaks corresponded to those in the reference sample within a tolerance of ±0.5%, as [55] states.

In addition, the loadings of the spectral profile matched the spectra obtained from the 400 μg L^{-1} sample used as reference, which helped to identify both BPA-d_{16} and BPA peaks. Unequivocal identification of both compounds was carried out by verifying that the relative abundances obtained from the loadings of the spectral profiles were within the estimated tolerance intervals shown in Table 1. This meant that the PARAFAC decomposition was capable of extracting and differentiating the information related to each one of the two analytes. The loadings of the sample profile for BPA increased throughout every experiment, whereas those for the internal standard BPA-d_{16} remained nearly constant.

Unequivocal identification of all the analyzed compounds was performed in the same way for the four experiments of the design. It was also confirmed that the relative retention times of the rest of peaks corresponded to those in the reference sample (data not shown in this work).

4.5. Optimization: figures of merit

Once PARAFAC decomposition was carried out for every analyte, the loadings of the sample profile of the factor related to the analyte were standardized by dividing each of them by the corresponding loading of the internal standard. Next, a regression model was built for each analyte at each experiment, so 16 calibration models were performed.

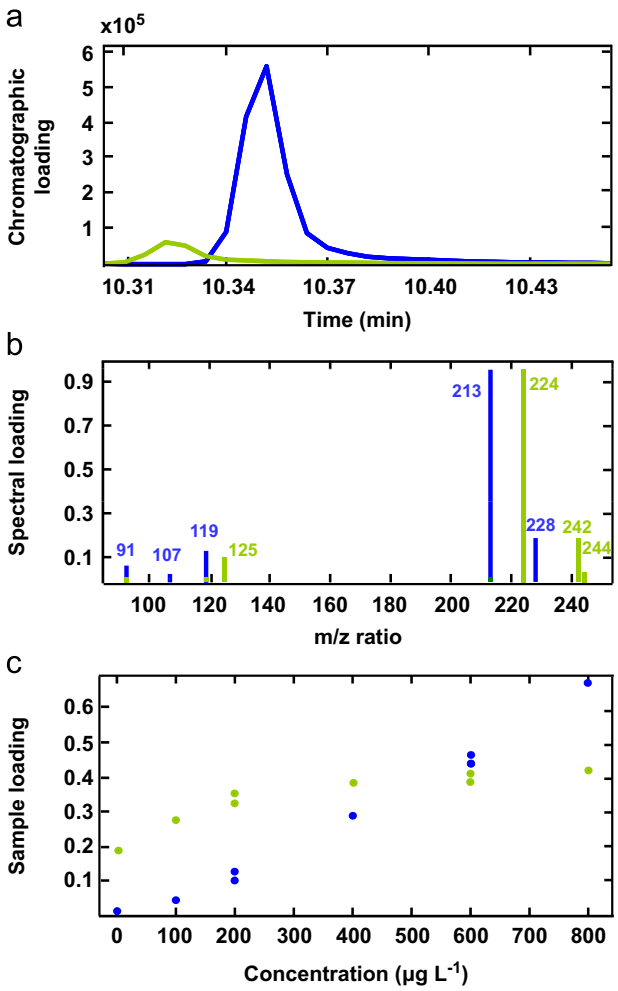

Fig. 3. Loadings of the: (a) chromatographic, (b) spectral and (c) sample profiles of the PARAFAC model for BPA-d_{16} and BPA corresponding to experiment 4. Factor 1 (BPA): dark blue; and factor 2 (BPA-d_{16}): light green. (For interpretation of the references to color in this figure legend, the reader is referred to the web version of this article.)

Table S1 of the "Electronic supplementary material" (ESM) contains all the data of the linear regressions "standardized loading versus true concentration" performed. It can be seen that a significant lack of fit was concluded in 10 out of 16 models. This drawback improved when a second-degree polynomial model was considered. In addition, in all cases, for the corresponding accuracy lines ("estimated concentration versus true concentration"), slope equal to 1 and intercept equal to 0 were obtained, i.e. at the 5% signification level, there was neither proportional nor constant bias, respectively. In Tables and Figs. S2 and S3 of the ESM both the linear and the second-order polynomial models for BFDGE from experiment 1 are shown.

From these regression models, five figures of merit were determined: (1) Precision (i.e. the residual standard deviation of the polynomial curves; s_{yx_load}); (2) Residual standard deviation of the accuracy line (s_{yx_accur}); (3) Decision limit, CCα, for a nominal value x_0 equal to 600 μg L^{-1} with the probability of false non-compliance, α, equal to 0.05; (4) Mean (ERRORm) and (5) Standard deviation (ERRORstd) of the absolute values of relative errors. In this way, for every studied temperature program, each analyte was identified through the PARAFAC decomposition previously detailed and the five figures of merit shown in Table 2.

4.6. Optimization: principal component analysis

The procedure followed to analyze the figures of merit for the four compounds altogether was based on a principal component analysis (PCA) of the data of Table 2 previously autoscaled. The cross-validation step was carried out by means of the "leave-one-out" technique. The lowest value of the root mean square error of cross-validation (RMSECV) was reached with the one-component model, which explained 93.13% of the variability of the data.

Fig. 4a shows the loadings of the PCA model performed, all of them positive. Therefore, the more similar and lower values of the four scores achieved with a temperature program, the better the analytical quality of the procedure, since better figures of merit would be then obtained. As the scores for BADGE in the experiments 1 and 3 (see Fig. 4b) were so high and positive, this meant that the quality of the determinations of this compound in those chromatographic conditions was poor. So they were rejected because suitable analytical quality would be desirable simultaneously for all the four analytes.

Between the other two oven temperature programs, none of them was especially appropriate for all the analytes in a simultaneous way. For the determination of BADGE, it would be clearly better to use the conditions of experiment 2, just like for that of BPF, but the temperature program of experiment 4 would be the best choice for the analysis of the other two analytes (Fig. 4b). The criterion used to decide which temperature program was the most suitable was based on the legislation currently in force. Thus, the oven temperature program finally selected was that of experiment 4 (ϕ_3=30 °C min^{-1} and ϕ_4=30 °C min^{-1}), because it made it possible to obtain the best figures of merit for BPA and BFDGE, both banned in certain cases. Furthermore, it meant the shortest total run time, which satisfied the third optimization criterion established in subsection "Optimization: experimental design".

4.7. Validation of the analytical procedure

Given that second-degree polynomial regressions were needed for fitting the calibration curves in subsection "Optimization: figures of merit", a reduction of the calibration range was realized. In this case, the concentration of the analytes ranged from 0 to 60 μg L^{-1}, whereas that of the internal standard remained constant at 8 μg L^{-1}. Sixteen calibration samples were analyzed at

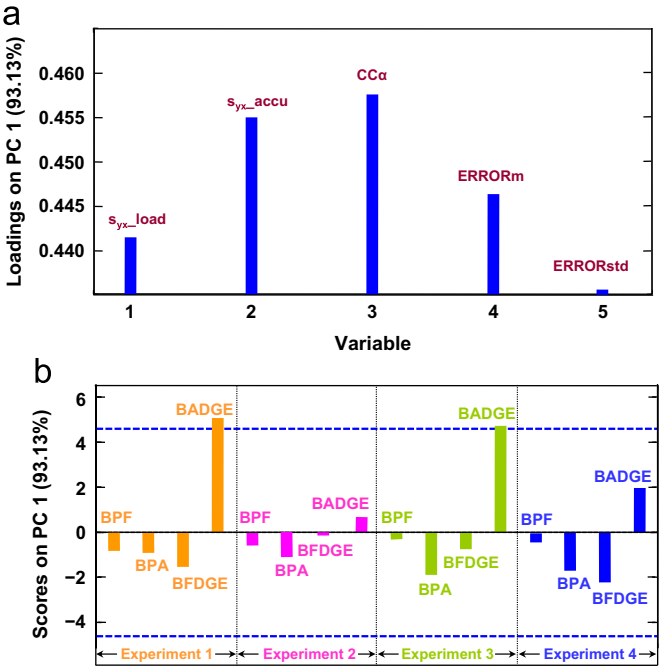

Fig. 4. (a) Loadings and (b) scores of the one-component PCA model. s_{yx_load}: residual standard deviation of the polynomial curves; s_{yx_accur}: residual standard deviation of the accuracy line; CCα: decision limit for a nominal value of 600 μg L^{-1} and a probability of false non-compliance equal to 0.05; ERRORm: mean of absolute values of relative errors; ERRORstd: standard deviation of absolute values of relative errors.

the chromatographic conditions of experiment 4. The MSD was operated in SIM mode, as detailed in subsection "GC/MS analysis". Thus, four new data tensors were obtained, whose dimensions were $16 \times 5 \times 22$ for BPF, $16 \times 9 \times 21$ for BPA-d_{16} and BPA (as previously, an only data tensor was considered for both analytes simultaneously), $16 \times 12 \times 20$ for BFDGE, and $16 \times 12 \times 17$ for BADGE.

From these data tensors, PARAFAC decompositions were carried out. Next, a linear least squares (LS) regression model "standardized loading versus true concentration" was performed for each analyte, and the corresponding accuracy line from it. Firstly, outlier data were detected using a robust regression by least median of squares (LMS) and then removed out of the calibration set if their absolute values of standardized residual and/or diagnostic resistance were higher than 2.5. The final PARAFAC models had one factor for BPF and BADGE, whereas for BPA-d_{16}, BPA and BFDGE two-factor models were needed, which achieved CORCONDIA values of 100%. In all cases, it was checked if the relative ratios of the loadings of the spectral profiles were within the established tolerance intervals, and it was concluded that all the analytes were unequivocally identified in this way.

The parameters of the accuracy line for each peak, along with the figures of merit related to it, are shown in Table 3; the number of outliers is shown in brackets. In all cases, the property of trueness was fulfilled. Values of capability of detection, CCβ, between 2.65 and 4.71 μg L^{-1} were achieved for probabilities of false positive (α) and false negative (β) equal to 0.05. The mean of the absolute values of relative errors ranged from 5.0 to 10.8%.

4.8. Application to food simulant samples: migration from PC tableware

At this stage of the work, a change of the injection solvent from acetonitrile to acetone was decided so as to extend the useful life of the GC/MS system. On the other hand, the capillary column was also replaced by a new one of the same type as the former.

It was verified firstly that the new solvent was evaporated properly in the PTV injector and that the GC/MS method optimized using now acetone as solvent was as suitable as it was for acetonitrile. The only change in the GC/MS method involved the four SIM acquisition windows, which had to be modified since the absolute retention times of the analytes had changed as a result of having installed a new column.

24 simulant food samples were analyzed, from which 13 samples, both spiked and non-spiked, came from the migration testing performed on some PC tableware (2 cups and 2 glasses). The 11 remaining samples were prepared from food simulant that had not been in contact with the PC containers; 5 out of these 11 samples were aimed at evaluating the repeatability of the analytical procedure, so each of them was fortified at a 200 ng L^{-1} concentration level of BPF, BPA, BFDGE and BADGE. This fortification level would mean a final concentration of 25 μg L^{-1} of every compound in the vial if a 100% of recovery was reached. As a result of the final reconstitution step, all these 24 simulant samples contained 10 μg L^{-1} of the internal standard. Table 4 collects these samples together with their origin and fortification level. 10 standards ranging from 0 to 40 μg L^{-1} of the four analytes (with 10 μg L^{-1} of the internal standard) were also prepared in acetone for assessing the recovery of the method.

Table 3
Parameters of the accuracy line and figures of merit determined for the four analytes. Linear calibration range: 0–60 μg L^{-1} for BPF, BPA, BFDGE and 0–8 μg L^{-1} for BADGE.

	BPF	BPA	BFDGE	BADGE
Number of standards (outliers)	16 (3)	16 (2)	16 (5)	5 (0)
b_0	3.01×10^{-9}	1.42×10^{-8}	2.68×10^{-4}	0.00
b_1	0.99	0.99	1.00	1.00
$s_{y/x}$	0.88	0.70	1.19	0.62
R^2 (%)	99.84	99.89	99.37	97.20
CCα (μg L^{-1})	1.90	1.50	2.42	2.48
CCβ (μg L^{-1})	3.34	2.65	4.71	3.50
MAE[a] (%)	5.53	5.04	10.85	8.16

[a] Mean of the absolute values of relative errors.

4.8.1. Tolerance intervals for the unequivocal identification of the analytes

Before quantifying, it is necessary to establish the tolerance intervals for the unequivocal identification of every analyte, as it is laid down in [55]. Replicated standards with concentrations of 6, 20 and 35 μg L^{-1} of BPF, BPA, BFDGE and BADGE in acetone (with 10 μg L^{-1} of the internal standard) were first analyzed and used as references at those three different concentration levels for the confirmation of the presence of every analyte according to its mass spectrum and relative retention time. In each case and taking the permitted maximum tolerances into account, the intervals for the diagnostic ions were estimated in the same way as in subsection "Initial approach: SIM mode".

A change in the most intense ion of BPF (m/z 107 or m/z 200) when either the 6 μg L^{-1} standard or the 20 μg L^{-1} and/or the 35 μg L^{-1} standard was considered was observed (see Table 5 – second column). This incongruous situation, which may be caused by the different contributions of the background noise to the mass spectrum at different concentration levels, led to the performance of the PARAFAC decomposition of a data tensor where the six matrices (reference standards) containing the data of the absolute intensities of the five characteristic m/z ratios for BPF at its elution range were included (tensor dimension $6 \times 5 \times 11$). The non-negativity constraint on both chromatographic and spectral ways was imposed, and a PARAFAC model with one factor was consequently obtained. This methodology enabled the extraction of the unique spectral profile of BPF as it was expected to be from

Table 4
Food simulant samples analyzed, indicating their fortification level and concentration of every analyte predicted from the linear regression "standardized sample loading versus true concentration". The symbol "—" denotes an outlier sample.

Container	Sample	Sample number[a]	Fortification level of BPF, BPA, BFDGE and BADGE (ng L^{-1})	c_{PRED} (BPF) (μg L^{-1})	c_{PRED} (BPA) (μg L^{-1})	c_{PRED} (BFDGE) (μg L^{-1})	c_{PRED} (BADGE) (μg L^{-1})
Glass flask 1	Repeatability 1	11	200[b]	17.27 ± 1.70	39.11 ± 2.77	0	0
Glass flask 2	Repeatability 2	12	200	14.85 ± 1.71	39.29 ± 1.34	4.31 ± 2.53	5.90 ± 3.4
Glass flask 3	Repeatability 3	13	200	12.94 ± 1.70	29.36 ± 1.24	12.70 ± 2.42	8.29 ± 3.37
Glass flask 4	Repeatability 4	14	200	10.49 ± 1.72	27.45 ± 1.23	14.61 ± 2.41	15.90 ± 3.36
Glass flask 5	Repeatability 5	15	200	13.14 ± 1.71	31.89 ± 1.26	0	0
Glass flask 6	Spiked 1–1st	16	200	13.23 ± 1.71	38.50 ± 2.78	4.58 ± 2.53	6.41 ± 3.39
Glass flask 7	Spiked 1–2nd	17	200	12.93 ± 1.71	—	7.53 ± 2.48	—
Glass flask 8	Spiked 2–1st	18	400[c]	25.04 ± 1.74	56.14 ± 2.66	12.99 ± 2.42	5.67 ± 3.4
Glass flask 9	Spiked 2–2nd	19	400	26.07 ± 1.74	62.76 ± 2.68	13.95 ± 2.42	7.96 ± 3.37
Glass flask 10	Non-spiked – 1st	20	0	—	—	0	0
Glass flask 11	Non-spiked – 2nd	21	0	0	—	0	0
PC cup 1	Spiked 1	22	200	17.53 ± 1.71	—	7.56 ± 2.48	0
	Spiked 2	23	400	41.05 ± 2.99	248.45 ± 33.75	19.71 ± 2.41	14.00 ± 3.35
	Non-spiked – 1st	24	0	0	227.93 ± 37.96	0	0
	Non-spiked – 2nd	25	0	0	225.73 ± 37.98	0	0
PC cup 2	Spiked 2	26	400	38.70 ± 3.02	276.32 ± 37.61	—	30.37 ± 3.67
	Non-spiked – 1st	27	0	0	263.94 ± 37.65	0	0
	Non-spiked – 2nd	28	0	0	160.75 ± 39.16	0	0
PC glass 1	Spiked 2	29	400	36.32 ± 3.05	228.10 ± 37.96	21.31 ± 2.41	11.02 ± 3.36
	Non-spiked – 1st	30	0	0	151.63 ± 39.38	0	0
	Non-spiked – 2nd	31	0	0	127.50 ± 40.04	0	0
PC glass 2	Spiked 2	32	400	37.02 ± 3.04	199.93 ± 38.35	23.56 ± 2.43	14.20 ± 3.35
	Non-spiked – 1st	33	0	0	168.59 ± 38.97	0	0
	Non-spiked – 2nd	34	0	0	121.76 ± 40.21	0	0

[a] In the tensor containing the calibration standards within the range 0–40 μg L^{-1}.
[b] Equivalent to 25 μg L^{-1} of every compound in vial if a 100% of recovery is reached.
[c] Equivalent to 50 μg L^{-1} of every compound in vial if a 100% of recovery is reached.

the experimentation already conducted (the base peak was m/z 200), so the tolerance intervals for the relative ion abundances could then be estimated. The comparison between the tolerance intervals for BPF obtained for each standard analyzed and those estimated from the PARAFAC decomposition performed are shown in Table 5. As long as the GC/MS data are trilinear, which guarantees the second-order advantage, if the common mass spectrum extracted from the PARAFAC decomposition of the data tensor of the standards at different concentrations is considered, a subjective choice of the reference mass spectrum will be avoided. If this strategy had not been followed, using as reference the mass spectrum obtained from one standard or another would have led to a high number of false negatives.

The same PARAFAC strategy was followed in the case of the other four compounds. In consequence, a two-factor model was fitted from the decomposition of the common tensor for BPA-d_{16} and BPA (dimension $6 \times 9 \times 15$), with a CORCONDIA value of 100%. For BFDGE, the best PARAFAC model estimated from the corresponding tensor, with dimension $6 \times 5 \times 17$, turned out to be the three-factor one, where the chromatographic, spectral and sample profiles showed all complete coherence, being the CORCONDIA index equal to 90%; a PARAFAC model with one factor was determined from the BADGE tensor (dimension $6 \times 5 \times 17$). The resultant tolerance intervals for the diagnostic ions of BPA-d_{16}, BPA, BFDGE and BADGE from the corresponding PARAFAC decomposition are gathered in Table 6. On the other hand, the tolerance intervals for the relative retention time of every analyte were also estimated in order to ensure its unequivocal identification as it is established in the European legislation ([39,55]) (data not shown in this work).

4.8.2. Quantification and identification in the food simulant samples

Next, PARAFAC decompositions of the four data tensors that comprised in each case the data matrices from both the 10 calibration standards and the 24 simulant food samples were performed with the chromatographic and spectral ways non-negativity-constrained. The dimensions of these four tensors were, respectively, $(34 \times 5 \times 18)$ for BPF; $(34 \times 9 \times 23)$ for the common tensor for BPA-d_{16} and BPA; $(34 \times 5 \times 30)$ for BFDGE; and $(34 \times 5 \times 25)$ for BADGE.

For BPF, a three-factor PARAFAC model (CORCONDIA value of 98%) was achieved after the removal of sample 20, which was considered as an outlier since its Q and T^2 indices exceeded their threshold values at the 99% confidence level. The loadings of the chromatographic, spectral and sample profiles of factor number 2 (in green dots in Fig. 5) were coherent with BPF; this enabled the unequivocal identification of this analyte (data not shown in this work). The other two factors were linked with unidentified non-target compounds derived from the simulant samples, since, as it is depicted in Fig. 5, they were only present in some of them.

In the case of the PARAFAC decomposition of the common tensor for BPA-d_{16} and BPA, the factor corresponding to the internal standard was not at first extracted, quite the opposite of what happened with BPA. This setback was put down to a

Table 5
Tolerance intervals for the five diagnostic ions for BPF estimated from the mass spectrum recorded at the retention time of every standard and from the PARAFAC decomposition of the tensor including the six standards at three different concentrations. The base peak in each case is in bold.

	m/z ratio	Abundance	Relative abundance (%)	Tolerance interval (%)
6 μg L^{-1} standard (1st replicate)	94	796	14.34	(11.47–17.21)
	107	4820	86.85	(78.16–95.53)
	152	973	17.53	(14.03–21.04)
	183	1553	27.98	(23.79–32.18)
	200	5550	**100**	–
6 μg L^{-1} standard (2nd replicate)	94	772	17.11	(13.69–20.53)
	107	4512	**100**	–
	152	707	15.67	(12.54–18.80)
	183	1185	26.26	(22.32–30.20)
	200	4357	96.56	(86.91–106.22)
20 μg L^{-1} standard (1st replicate)	94	5848	17.03	(13.62–20.43)
	107	34344	**100**	–
	152	5560	16.19	(12.95–19.43)
	183	7089	20.64	(17.55–23.74)
	200	30072	87.56	(78.81–96.32)
20 μg L^{-1} standard (2nd replicate)	94	4423	12.63	(10.10–15.15)
	107	27080	77.32	(69.59–85.05)
	152	4679	13.36	(10.69–16.03)
	183	7202	20.56	(17.48–23.65)
	200	35024	**100**	–
35 μg L^{-1} standard (1st replicate)	94	10158	17.51	(14.01–21.01)
	107	58016	**100**	–
	152	9418	16.23	(12.99–19.48)
	183	11474	19.78	(15.82–23.73)
	200	49304	84.98	(76.49–93.48)
35 μg L^{-1} standard (2nd replicate)	94	14991	16.79	(13.43–20.15)
	107	74368	83.29	(74.96–91.62)
	152	13622	15.26	(12.21–18.31)
	183	17856	20.00	(16.00–24.00)
	200	89288	**100**	–
PARAFAC decomposition ($6 \times 5 \times 11$ tensor)[a]	94	0.111	15.12	(12.09–18.14)
	107	0.643	87.75	(78.97–96.52)
	152	0.111	15.12	(12.10–18.15)
	183	0.157	21.36	(18.16–24.57)
	200	0.733	**100**	–

[a] For the determination of the tolerance intervals, the spectral loadings were used.

numeric effect because of the large chromatographic and sample loadings of the factor matched BPA. As the characteristic m/z ratios for the detection of BPA-d_{16} were specific and different from those chosen for BPA, this problem could be solved by dividing the original tensor including BPA-d_{16} and BPA data into two new tensors: the BPA-d_{16} one, which contained the first 11 elution times of the former tensor (dimension $34 \times 9 \times 11$), and the other for BPA, with dimension $34 \times 9 \times 12$.

On the one hand, the PARAFAC decomposition of the first new tensor produced a 4-factor model (CORCONDIA value of 87%) without having detected any outliers. The loadings of the chromatographic, spectral and sample profiles of factor number 2 matched BPA-d_{16}, while those of factor number 1 did BPA, since this analyte coeluted in the range of times used for constructing the BPA-d_{16} tensor. The other two factors could not be identified and, as in the previous case, were regarded as interferents only encountered in some simulant samples. From that PARAFAC model estimated, the presence of the internal standard was unequivocally confirmed. It must be noticed that this unequivocal identification together with the quantification of this compound could never have been achieved from the TIC of most simulant samples analyzed, because in that case those two non-target compounds, especially the one associated with factor number 3, concealed the presence of BPA-d_{16} to such an extent that the mass spectrum extracted from the TIC at the retention time of this compound did not match what was expected for it at all. This is illustrated in Fig. 6, where Fig. 6a collects the chromatographic profile resultant from the PARAFAC decomposition of the BPA-d_{16} tensor into 4 factors, and Fig. 6b represents the spectral profile of the factor 2, identified as BPA-d_{16}; these two graphics contrast with Fig. 6c and d, being the former one the TIC obtained for one of the samples analyzed in the same range of time as Fig. 6a, while the latter reflects the mass spectrum registered at 10.508 min, the retention time of BPA-d_{16}. The mass spectrum in Fig. 6d is clearly different from that of BPA-d_{16}, which appears in Fig. 6b and is detailed in Table 6.

On the other hand, BPA was both unequivocally identified and quantified from a 3-factor model resulting from the PARAFAC decomposition of the second new tensor. The CORCONDIA index equaled 100% and no outliers were detected. The first factor (in blue dots in Fig. 7a and b) was coherent with BPA, while the other two remained unknown again.

When the PARAFAC decomposition of the BFDGE tensor was performed, a numeric effect was again detected, and the factor for this analyte could not be extracted. After the division of the original tensor to obtain a new one (with dimension $34 \times 5 \times 18$) where the greatest factor (an unidentified interferent) in the former decomposition was only partly included, a 3-factor model was estimated from the PARAFAC decomposition of this new BFDGE tensor (CORCONDIA value of 99%). One outlier object, sample 26, was removed. It was verified that the loadings of the three profiles of the factor number 3 matched *p*–*p*′ BFDGE, so this analyte was unequivocally identified.

In the case of BADGE, the PARAFAC decomposition of its corresponding tensor yielded a 2-factor model (CORCONDIA index of 91%). Sample 17 was rejected as an outlier. Factor 1 was coherent with the chromatographic, spectral and sample profiles expected for BADGE, and its correct identification was ensured from it.

The fact that the number of factors in the PARAFAC models when both standards and samples were included in the data tensors was greater than that when only standards were is remarkable. That increase may be due to the coelution of

Table 6
Tolerance intervals for the diagnostic ions for BPA-d_{16}, BPA, BFDGE and BADGE estimated from the PARAFAC decomposition of the corresponding tensor including the six standards at three different concentrations. The base peak in each case is in bold.

Analyte	m/z ratio	Abundance	Relative abundance (%)	Tolerance interval (%)
BPA-d_{16}	125	2.03×10^{-1}	21.04	(17.89–24.20)
($6 \times 9 \times 15$ tensor)	**224**	9.63×10^{-1}	**100**	–
	242	1.75×10^{-1}	18.15	(14.52–21.78)
	244	2.71×10^{-3}	0.28	(0.14–0.42)
BPA	91	8.27×10^{-2}	8.56	(4.28–12.84)
($6 \times 9 \times 15$ tensor)	107	3.90×10^{-2}	4.04	(2.02–6.06)
	119	1.48×10^{-1}	15.31	(12.25–18.37)
	213	9.66×10^{-1}	**100**	–
	228	1.90×10^{-1}	19.69	(15.75–23.62)
BFDGE	107	2.76×10^{-1}	36.59	(31.10–42.08)
($6 \times 5 \times 17$ tensor)	181	4.54×10^{-1}	60.21	(54.19–66.23)
	197	7.54×10^{-1}	**100**	–
	279	1.60×10^{-2}	2.12	(1.06–3.18)
	312	3.87×10^{-1}	51.40	(46.26–56.54)
BADGE	91	3.51×10^{-2}	3.56	(1.78–5.34)
($6 \times 5 \times 17$ tensor)	119	5.07×10^{-2}	5.14	(2.57–7.70)
	169	2.35×10^{-2}	2.38	(1.19–3.57)
	325	9.86×10^{-1}	**100**	–
	340	1.51×10^{-1}	15.25	(12.20–18.30)

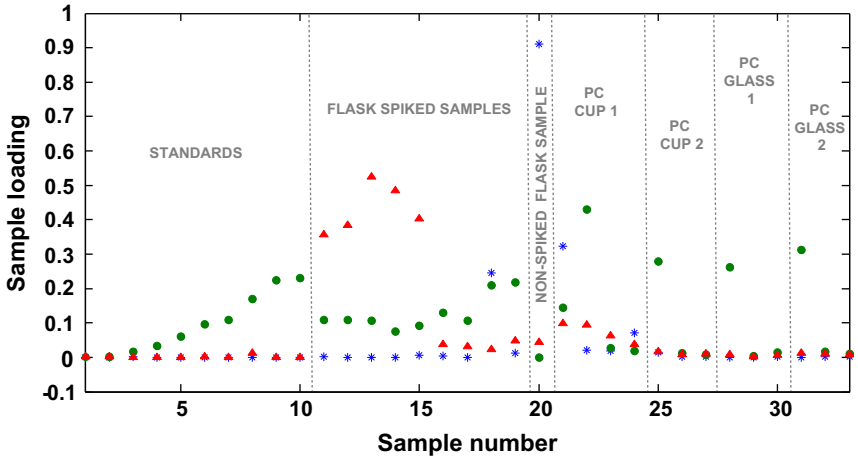

Fig. 5. Sample loadings for the three factors resultant from the PARAFAC decomposition of the BPF tensor including standards (from 0 to 40 μg L^{-1}) and the samples in Table 4, which has been renumbered because the sample 20 has not been taken into consideration for the analysis. Factor 1, in blue asterisks; factor 2 (BPF), in green dots; factor 3, in red triangles. (For interpretation of the references to color in this figure legend, the reader is referred to the web version of this article.)

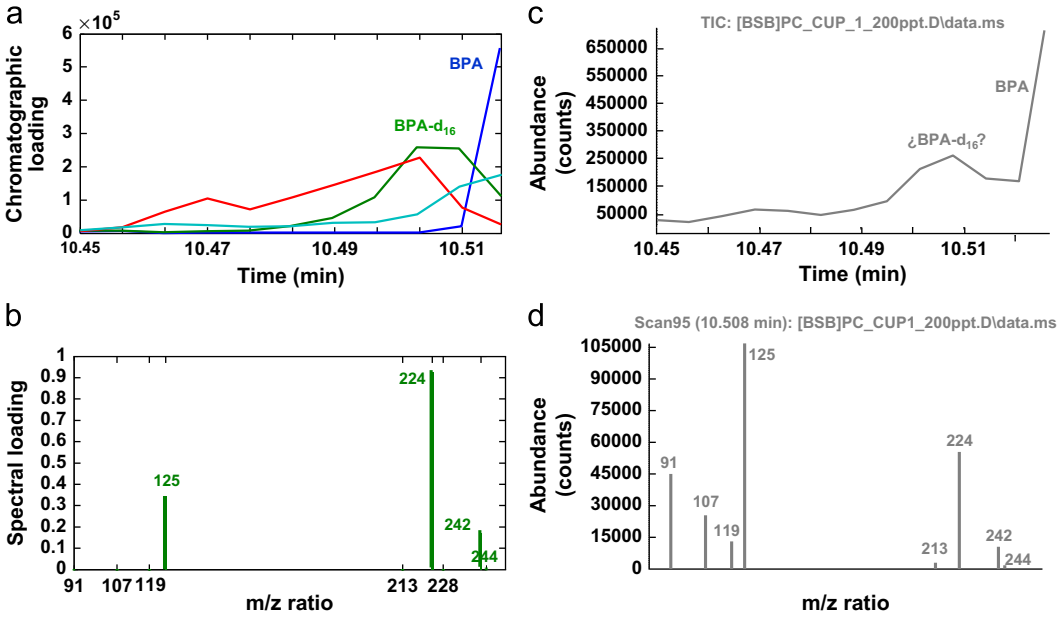

Fig. 6. Chromatographic and spectral data derived from the PARAFAC decomposition of the BPA-d_{16} tensor and those from the original TIC registered for one of the samples. (a) Loadings of the chromatographic profiles of the 4-factor PARAFAC model; factor 1 (in blue) matched BPA, while factor 2 (in green) did BPA-d_{16}. (b) Loadings of the spectral profile for the factor 2. (c) Enlarged TIC of the simulant sample 22 (see Table 4) within the elution zone of BPA-d_{16}. (d) Mass spectrum registered at the maximum of the peak considered as BPA-d_{16}. (For interpretation of the references to color in this figure legend, the reader is referred to the web version of this article.)

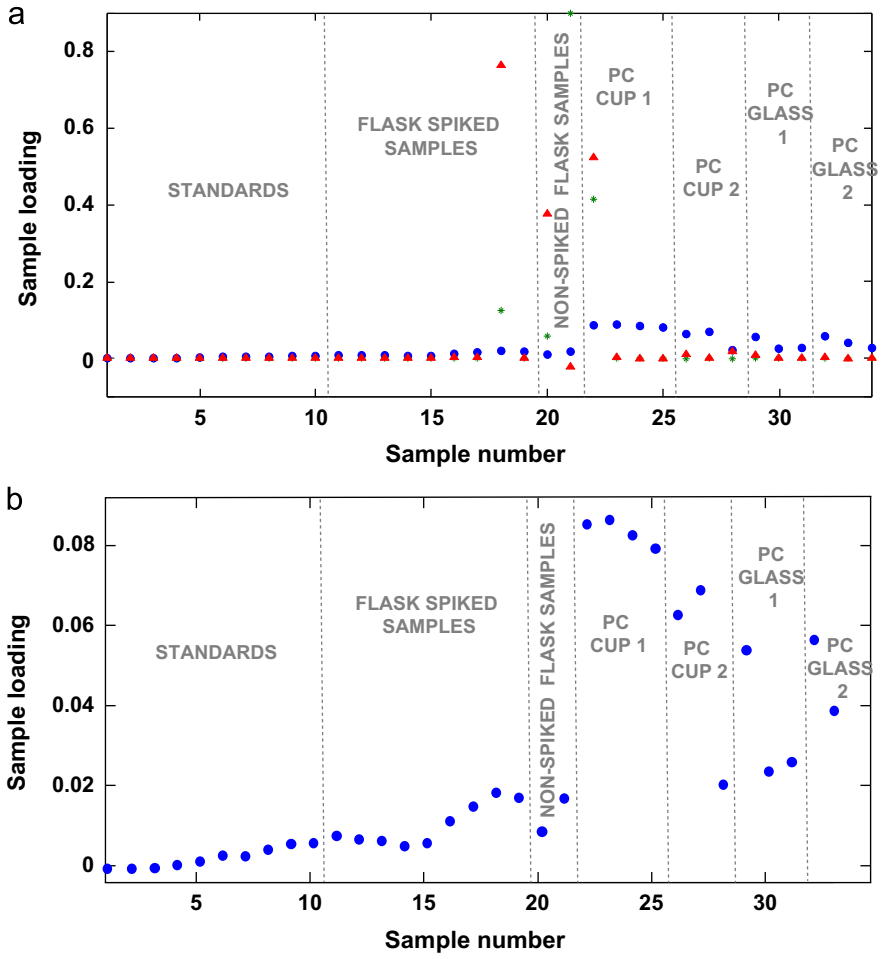

Fig. 7. Sample loadings from the PARAFAC decomposition of the BPA tensor including standards (from 0 to 40 μg L^{-1}) and the samples in Table 4. (a) The three factors. Factor 1 (BPA), in blue dots; factor 2, in green asterisks; factor 3, in red triangles. (b) Only the factor 1. (For interpretation of the references to color in this figure legend, the reader is referred to the web version of this article.)

Table 7
Results of the LMS and LS regressions "standardized sample loading versus true concentration" performed.

Analyte	Calibration range ($\mu g\ L^{-1}$)	LMS regression			LS regression				
		Model	Outlier ratio	Model (R^2; s_{yx})	n	Hypothesis test	p-value	MAE in calibr.[f]	MAE in pred.[g]
BPF	0–40	$y=9.00\times10^{-3}+4.28\times10^{-2}x$	0/10	$y=-7.68\times10^{-3}+4.27\times10^{-2}x$ (99.78%; 3.01×10^{-2})	10	F-test[a]	0.00	5.54%	Not estimated
						χ^2 test[b]	0.33		
						S-W test[c]	0.05		
						K-S test[d]	0.87		
						D-W test[e]	0.50		
	30–90	$y=-0.23+3.05\times10^{-2}x$	2/7	$y=-0.23+3.0\times10^{-2}x$ (99.90%; 2.57×10^{-2})	5	F-test	0.00	0.94%	2.14%
						χ^2 test	Not computed		
						S-W test	0.58		
						K-S test	0.23		
						D-W test	0.63		
BPA	0–40	$y=3.00\times10^{-3}+1.13\times10^{-3}x$	2/10	$y=2.50\times10^{-3}+1.15\times10^{-3}x$ (99.94%; 4.99×10^{-4})	8	F-test	0.00	6.39%	Not estimated
						χ^2 test	0.35		
						S-W test	0.14		
						K-S test	0.62		
						D-W test	0.56		
	30–90	$y=-9.97\times10^{-2}+2.37\times10^{-2}x$	1/7	$y=-0.14+2.43\times10^{-2}x$ (99.88%; 2.15×10^{-2})	6	F-test	0.00	1.34%	10.59%
						χ^2 test	Not computed		
						S-W test	0.73		
						K-S test	0.94		
						D-W test	0.14		
	100–650	$y=-8.75\times10^{-2}+3.90\times10^{-3}x$	3/7	$y=-8.49\times10^{-2}+3.89\times10^{-3}x$ (99.92%)	4	F-test	0.00	2.72%	7.02%
						χ^2 test	0.17		
						S-W test	0.85		
						K-S test			
						D-W test	0.09		
BFDGE	0–40	$y=1.05\times10^{-1}+6.35\times10^{-2}x$	1/10	$y=1.25\cdot10^{-1}+6.40\times10^{-2}x$ (99.56%; 6.18×10^{-2})	9	F-test	0.00	5.76%	Not estimated
						χ^2 test	0.42		
						S-W test	0.25		
						K-S test	0.77		
						D-W test	0.72		
BADGE	0–40	$y=4.35\times10^{-2}+6.21\times10^{-2}x$	2/10	$y=6.98\times10^{-2}+6.30\times10^{-2}x$ (99.31%; $8.13\cdot10^{-2}$)	8	F-test	0.00	8.77%	Not estimated
						χ^2 test	0.12		
						S-W test	0.02		
						K-S test	0.39		
						D-W test	0.51		

[a] Test for the significance of the regression, where H_0: the regression model is not statistically significant.
[b] Chi-square test, where H_0: residuals are compatible with a normal distribution.
[c] Shapiro-Wilk test, where H_0: residuals are compatible with a normal distribution.
[d] Kolmogorov-Smirnov test, where H_0: residuals are compatible with a normal distribution.
[e] Durbin-Watson test, where H_0: residuals are not autocorrelated.
[f] Mean of the absolute value of the relative errors in calibration.
[g] Mean of the absolute value of the relative errors in prediction.

Table 8
Analysis of trueness and values of the decision limit and detection capability.

Analyte	Calibration range ($\mu g\ L^{-1}$)	LS regression "predicted concentration versus true concentration"				CCα; CCβ ($\mu g\ L^{-1}$)
		n	Model (R^2; s_{yx})	p-value for the test $b_0=0$	p-value for the test $b_1=1$	
BPF	0–40	10	$y=0.0+1.0x$ (99.78%; 7.05×10^{-1})	1.0	1.0	2.85; 2.90[a]
	30–90	5	$y=4.72\times10^{-5}+1.0x$ (99.90%; 8.40×10^{-1})	0.99	0.99	–
BPA	0–40	8	$y=4.82\times10^{-5}+9.99\times10^{-1}\,x$ (99.94%; $4.35\cdot10^{-1}$)	0.99	0.99	1.968; 1.969[a]
	30–90	6	$y=0.0+1.0x$ (99.88%; 8.86×10^{-1})	1.0	1.0	–
	100–650	4	$y=0.0+1.0x$ (99.92%; 7.82)	1.0	1.0	630.3; 657.2[b]
BFDGE	0–40	9	$y=2.32\times10^{-4}+9.99\times10^{-1}x$ (99.56%; 9.65×10^{-1})	0.99	0.99	4.07; 4.17[a]
BADGE	0–40	8	$y=1.11\times10^{-4}+9.99\times10^{-1}x$ (99.31%; 1.29)	0.99	0.99	5.40; 5.53[a]

[a] For a nominal value $x_0=0$, $\alpha=\beta=0.05$.
[b] For a nominal value $x_0=600\ \mu g\ L^{-1}$, $\alpha=\beta=0.05$.

interferents that were present in some samples. The injection volume of 10 μL may have also contributed to this situation, since the more sample volume injected, the higher the risk of coelution. However, what could have meant a severe problem in the identification and quantification of the analytes did not, because in all cases PARAFAC succeeded in extracting the factor associated to every analyte

correctly, even in the presence of coeluents. This allowed the unequivocal identification of all the compounds to be verified.

After the decomposition of every data tensor into the appropriate number of factors and the identification of the factor related to each compound, the sample-mode loadings of every analyte were standardized with the sample-mode loadings of the internal standard. In each case, a linear LS regression between the standardized sample-mode loadings and the concentration of the corresponding analyte in the calibration standards was performed for the quantification stage. Previously, a LMS regression was carried out to detect possible outlier data. A new LS regression "standardized sample-mode loading versus true concentration" was then estimated and validated.

The standardized sample-mode loading of some samples for BPF and/or BPA was greater than that of the 40 $\mu g\,L^{-1}$ standard, so two new sets of calibration standards (from 30 to 90 $\mu g\,L^{-1}$ of BPF and BPA and from 100 to 650 $\mu g\,L^{-1}$ of BPA) were prepared and analyzed in order to avoid extrapolation when determining the concentration of those samples. The second new calibration range was aimed at quantifying that analyte in all the PC samples. Therefore, three new tensors were built including in each case the new standards and only the samples that were out of the original calibration range: one for BPF, with dimension $13 \times 5 \times 18$ (9 standards from 30 to 90 $\mu g\,L^{-1}$, together with 4 samples); and the other two for BPA, with dimension (i) $15 \times 9 \times 12$ (9 standards from 30 to 90 $\mu g\,L^{-1}$, together with 6 samples) and (ii) $22 \times 9 \times 12$ (9 standards from 100 to 650 $\mu g\,L^{-1}$, together with the 13 PC samples). In these three new data tensors, two standards were aimed at estimating the relative error in prediction. A PARAFAC decomposition of each of these three tensors was then performed, and again, from the relative ratios of the loadings of the spectral profiles and from the relative retention time, it was verified that both BPF and BPA were unequivocally identified. New LMS and LS regressions were estimated from the corresponding PARAFAC model. The results of all the LMS and LS regressions built and the *p*-values for the hypothesis tests posed to validate every model are listed in Table 7. The mean of the absolute value of the relative errors, both in calibration (from 0.9% to 5.5%) and in prediction (from 2.1% to 10.6%), also figures on this table.

Two hypothesis tests enabled to verify the trueness of every calibration model by checking if, at the 95% significance level, there were no statistically significant differences between the values obtained, respectively, for the slope and 1, and the intercept and 0, of a linear LS regression "estimated concentration versus true concentration". The equations of all the trueness lines and the *p*-values for these last two hypothesis tests are collected in Table 8.

The detection capability for every analyte was determined for probabilities of false positive (α) and false negative (β) equal to 0.05, so values between 1.97 and 5.53 $\mu g\,L^{-1}$ were achieved (see Table 8, last column). The detection capability regarding the specific migration limit of 0.6 $mg\,kg^{-1}$ established for BPA in [18] was also calculated. As a result, CCα equaled 630.3 $\mu g\,L^{-1}$ and CCβ, 657.2 $\mu g\,L^{-1}$, which meant that the GC/MS method was able to distinguish 657.2 from 600 $\mu g\,L^{-1}$ with probabilities of false non-compliance and false compliance equal to 0.05.

The LS calibration models (see Table 7) enabled to determine the quantity of every analyte in every food simulant sample. The values of the concentration of every analyte in the 24 final simulant samples are shown in the last four columns of Table 4. On the other hand, the repeatability and the recovery of the method regarding every analyte were also estimated. The first performance characteristic was calculated in all cases as the standard deviation of the concentration of every analyte in the five repeatability simulant samples; in this way, the value for the repeatability standard deviation was 2.80 for BPF, 5.53 for BPA, 6.95 for BFDGE and 6.62 for BADGE. Recovery was expressed as the percentage of the amount initially added at every spiked sample that was recovered at last. The average recovery rates appear in Table 9. It must be noticed that, in general, better recoveries were obtained when the food simulant had been previously in contact with a PC container. On the other hand, the sample preparation method clearly performed better for BPF and BPA than for BFDGE and BADGE, as recoveries were higher for the first. This is the reason why the SPE step in this method is being optimized.

Table 9
Recovery rates of every analyte at the two fortification levels considered.

Analyte	Recovery rate (%)			
	Fortification level of 200 ng L^{-1}		Fortification level of 400 ng L^{-1}	
	Samples not in contact with PC tableware	Samples in contact with PC tableware	Samples not in contact with PC tableware	Samples in contact with PC tableware
BPF	55.17	70.13	51.11	76.55
BPA	149.57	–	125.53	113.95
BFDGE	24.99	30.23	26.94	43.06
BADGE	24.34	0	13.63	34.80

It was confirmed that the migration of BPA from the new PC containers into the food simulant had occurred, since the concentration of BPA in every PC non-spiked sample was different from 0. To be exact, the average BPA concentration in the simulant volume analyzed was 181.46 $\mu g\,L^{-1}$ for Cup 1, 148.64 $\mu g\,L^{-1}$ for Cup 2, 104.67 $\mu g\,L^{-1}$ for Glass 1, and 108.88 $\mu g\,L^{-1}$ for Glass 2. Bearing in mind the concentration factor and the recovery rate (113.95%), the average BPA concentration migrated from every PC container was 1.27 $\mu g\,L^{-1}$, 1.04 $\mu g\,L^{-1}$, 0.73 $\mu g\,L^{-1}$, and 0.76 $\mu g\,L^{-1}$, respectively. None of these values exceeded the specific migration limit laid down for BPA (0.6 $mg\,kg^{-1}$) in [18] on plastic materials and articles intended to come into contact with food.

Acknowledgments

Authors thank the financial support via projects Ministerio de Economía y Competitividad CTQ2011–26022 and JCyL BU108A11–2. M.L. Oca is particularly grateful to Universidad de Burgos for her FPI Grant.

Appendix A. Supporting information

Supplementary data associated with this article can be found in the online version at http://dx.doi.org/10.1016/j.talanta.2012.10.086.

References

[1] D. Arroyo, M.C. Ortiz, L.A. Sarabia, J. Chromatogr. A 1218 (2011) 4487–4497.
[2] R. Bro, Crit. Rev. Anal. Chem. 36 (2006) 279–293.
[3] M.C. Ortiz, L.A. Sarabia, J. Chromatogr. A 1158 (2007) 94–110.
[4] V. Gómez, M.P. Callao, Anal. Chim. Acta 627 (2008) 169–183.
[5] R. Bro, N. Viereck, M. Toft, H. Toft, P.I. Hansen, S.B. Engelsen, Trends Anal. Chem. 29 (2010) 281–284.
[6] L. Rubio, L.A. Sarabia, A. Herrero, M.C. Ortiz, Anal. Bioanal. Chem. 403 (2012) 1131–1143.
[7] R. Morales, M.C. Ortiz, L.A. Sarabia, Anal. Bioanal. Chem. 403 (2012) 1095–1107.
[8] D. Arroyo, M.C. Ortiz, L.A. Sarabia, J. Chromatogr. A 1157 (2007) 358–368.
[9] A. Guart, F. Bono-Blay, A. Borrell, S. Lacorte, Food Addit. Contam. 28 (2011) 1–10.
[10] W.F. Smith, Foundations of Materials Science and Engineering, fourth ed., McGraw-Hill, New York, 2005.
[11] A. Ballesteros-Gómez, F.J. Ruiz, S. Rubio, D. Pérez-Bendito, Anal. Chim. Acta 603 (2007) 51–59.
[12] J. Simal-Gandara, P. López Mahía, P. Paseiro Losada, J. Simal Lozano, S. Paz Abuín, Food Addit. Contam. 10 (1993) 555–565.

[13] T. Yamamoto, A. Yasuhara, Chemosphere 38 (1999) 2569–2576.
[14] R. Gachter, H. Muller, Plastic Additives Handbook, Hanser, New York, 1990.
[15] K.A. Mountfort, J. Kelly, S.M. Jickells, L. Castle, Food Addit. Contam. 14 (1997) 737–740.
[16] K.A. Ehlert, C.W.E. Beumer, M.C.E. Groot, Food Addit. Contam. 25 (2008) 904–910.
[17] A.G. Cabado, S. Aldea, C. Porro, G. Ojea, J. Lago, C. Sobrado, J.M. Vieites, Food Chem. Toxicol. 46 (2008) 1674–1680.
[18] Commission Regulation (EU) No. 10/2011 of 14 January 2011 on plastic materials and articles intended to come into contact with food. Off. J. Eur. Union L12,1–89.
[19] A. Ballesteros-Gómez, S. Rubio, D. Pérez-Bendito, J. Chromatogr. A 1216 (2009) 449–469.
[20] E. Ferrer, E. Santoni, S. Vittori, G. Font, J. Mañes, G. Sagratini, Food Chem. 126 (2011) 360–367.
[21] B. Shao, H. Han, D. Li, Y. Ma, X. Tu, Y. Wu, Food Chem. 105 (2007) 1236–1241.
[22] J.E. Biles, T.P. McNeal, T.H. Begley, H.C. Hollifield, J. Agric. Food Chem. 45 (1997) 3541–3544.
[23] J. López-Fernández, P. Paseiro-Losada, Food Addit. Contam. 20 (2003) 596–606.
[24] M. Del Olmo, A. González-Casado, N.A. Navas, J.L. Vílchez, Anal. Chim. Acta 346 (1997) 87–92.
[25] D.A. Markham, D.A. Mcnett, J.H. Birk, G.M. Klecka, M.J. Bartels, C.A. Staples, Int. J. Environ. Anal. Chem. 69 (1998) 83–98.
[26] A.K. Malik, C. Blasco, Y. Picó, J. Chromatogr. A 1217 (2010) 4018–4040.
[27] N. De Coensel, F. David, P. Sandra, J. Sep. Sci. 32 (2009) 3829–3836.
[28] P. Viñas, N. Campillo, N. Martínez-Castillo, M. Hernández-Córdoba, Anal. Bioanal. Chem. 397 (2010) 115–125.
[29] J.D. Stuart, C.P. Capulong, K.D. Launer, X. Pan, J. Chromatogr. A 1079 (2005) 136–145.
[30] N. Rastkari, R. Ahmadkhaniha, M. Yunesian, L.J. Baleh, A. Mesdaghinia, Food Addit. Contam. 27 (2010) 1460–1468.
[31] E. Hoh, K. Mastovska, J. Chromatogr. A 1186 (2008) 2–15.
[32] A.C. Heiden, B. Kolahgar, E. Pfannkoch, GERSTEL AppNote 7/2001, GERSTEL GmbH & Co. KG, Mülheim an der Ruhr. Available from: 〈http://www.gerstel.com/pdf/p-gc-an-2001-07.pdf〉 (accessed 29.07.11).
[33] C.A. Andersson, R. Bro, Chemom. Intell. Lab Syst. 52 (2000) 1–4.
[34] R. Bro, Chemom. Intell. Lab Syst. 46 (1999) 133–147.
[35] R.B. Catell, Psychometrika 9 (1944) 267–283.
[36] R. Bro, Ph.D. Thesis, Royal Veterinary and Agricultural University, Denmark, 1998.
[37] R. Bro, H.A.L. Kiers, J. Chemom. 17 (2003) 274–286.
[38] T. Pihlström, Method validation and quality control procedures for pesticide residues analysis in food and feed (SANCO/10684/2009). EU, Brussels, 2010.
[39] Commission Decision (EC) No. 2002/657/EC of 12 August 2002, Brussels, implementing Council Directive 96/23/EC concerning the performance of analytical methods and the interpretation of results, Off. J. Eur. Commun. L221 (17 August) 8–36.
[40] International Standard ISO 11843, Capability of detection, Geneva, Switzerland, Part 1, Terms and definitions, 1997 and Part 2, Methodology in the linear calibration case, 2000.
[41] J. Inczédy, T. Lengyel, A.M. Ure, A. Gelencsér, A. Hulanicki, Compendium of Analytical Nomenclature IUPAC, third ed., Pot City Press Inc, Baltimore, 2000.
[42] BIPM, IEC, IFCC, ILAC, IUPAC, IUPAP, ISO, OIML. International vocabulary of metrology - Basic and general concepts and associated terms (VIM), 3rd ed., JCGM 200:2012, 〈http://www.bipm.org/vim〉.
[43] IUPAC, Spectrochim. Acta B 33 (1978) 241–245.
[44] L.A. Currie, Anal. Chim. Acta 391 (1999) 127–134.
[45] C.A. Clayton, J.W. Hines, P.D. Elkins, Anal. Chem. 59 (1987) 2506–2514.
[46] L.A. Sarabia, M.C. Ortiz, TrAC, Trends Anal. Chem. 13 (1994) 1–6.
[47] M.C. Ortiz, M.S. Sánchez, L.A. Sarabia, in: S. Brown, R. Tauler, B. Walczak B (Eds.), Comprehensive Chemometrics, vol. 1, Elsevier, Oxford, 2009.
[48] M.C. Ortiz, L.A. Sarabia, I. García, D. Giménez, E. Meléndez, Anal. Chim. Acta 559 (2006) 124–136.
[49] M.C. Ortiz, L. Sarabia, M.S. Sánchez, Anal. Chim. Acta 674 (2010) 123–142.
[50] NIST Mass Spectral Search Program for the NIST/EPA/NIH Mass Spectral Library Version 2.0 a. build July 1 2002.
[51] B.M. Wise, N.B. Gallagher, R. Bro, J.M. Shaver, W. Windig, R.S. Koch, PLS Toolbox 5.0 Eigenvector Research, Inc. 3905 West Eaglerock Drive, Wenatchee, 2006.
[52] STATGRAPHICS Centurion XVI (Version 16.1.11), StatPoint Technologies, Inc., Herndon, VA, 2010.
[53] P.J. Rousseeuw, A.M. Leroy, Robust Regression and Outliers Detection, John Wiley and Sons, New Jersey, 2001.
[54] R. Sendón García, C. Pérez Lamela, P. Paseiro Losada, Rapid Commun. Mass Spectrom. 19 (2005) 1569–1574.
[55] Guidelines for performance criteria and validation procedures of analytical methods used in controls of food contact materials, EUR 24105 EN—first ed. 2009.